

Supporting Information

Precise Molecular Design for Twisted Thiophene-Based Mechanofluorochromic Probe with Large Stokes Shift and Feasibility Study Towards Security Ink and Re-writable Papers

Ram Prasad Bhatta,^a Sumit,^a Vishal Kachwal,^a Vandana Vishwakarma,^b Angshuman Roy Churudhury^b and Inamur Rahaman Laskar^{*a}

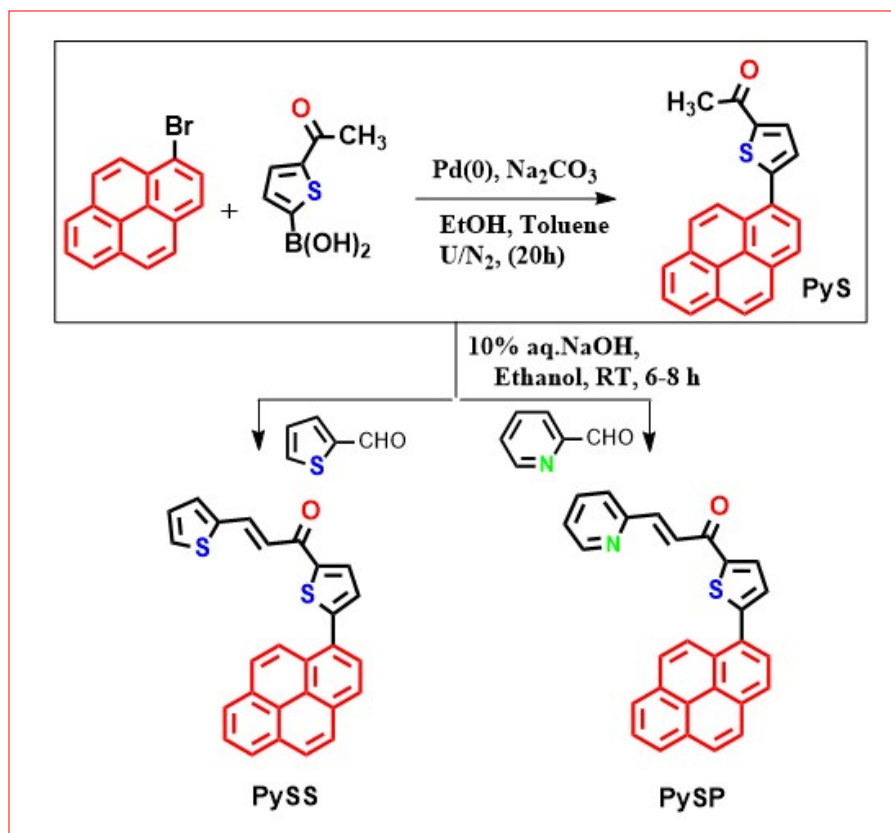
Email ir_laskar@pilani.bits-pilani.ac.in

[a] Department of Chemistry, Birla Institute of Technology and Science (BITS), Pilani Campus, Pilani, Rajasthan 333031, India.

[b] Department of Chemical Sciences, Indian Institute of Science Education and Research (IISER), Sector 81, S. A. S. Nagar, Manauli PO, Mohali, Punjab 140306, India.

Synthesis of PySS and PySP

The synthetic scheme of pyrene thiophene-based compounds is summarized in scheme S1. Initially, 1-(5-(Pyren-1-yl)thiazol-2-yl)ethan-1-one (PyS) was synthesized by using an earlier method reported by our group.¹ For the second step, compound (PySS), PyS (0.3 gm, 0.92 mmol) in ethanol (4 ml) was stirred for 30 min at 50 °C and cooled to (10-15) °C, then to a clear solution of reaction mass NaOH (10% aq. solution, 1ml) was added slowly and further stirred the reaction mass for 10-15 min then added thiophene-2-aldehyde (0.155 gm, 1.38 mmol). Then the reaction mass was stirred for 10-12 hr at 40-50 °C. Then it was cooled slowly to RT. Then, water (3 ml) was added which resulted in precipitate formation, filtered the reaction mass, was washed with chilled ethanol, and dried the obtained product for 12 hr. under vacuum. A dried product (350 mg, 90 % yield) was obtained. A similar process was followed to synthesize PySP. The synthesized compound was characterized by NMR and HRMS (Figure S1 to S9).



Scheme-S1. Synthetic route for the compounds (PySS and PySP)

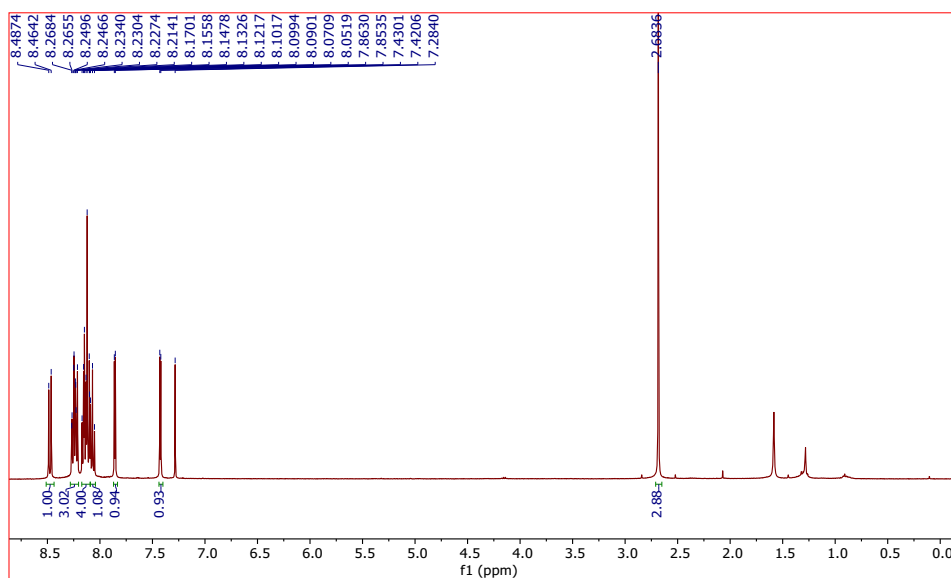


Figure S1. ^1H NMR spectra of PyS in CDCl_3 solvent

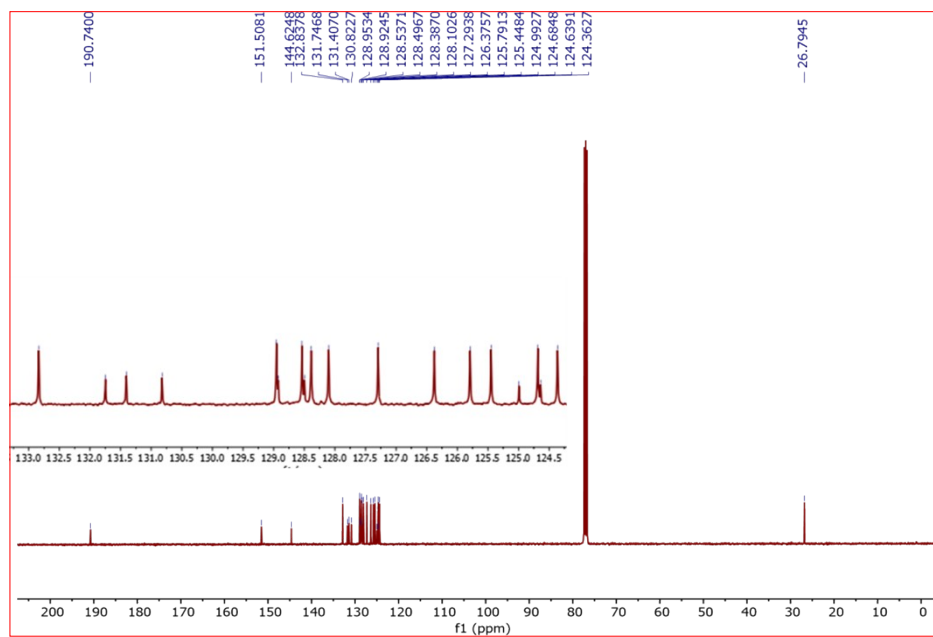


Figure S2. ^{13}C NMR spectra of PyS in CDCl_3 solvent

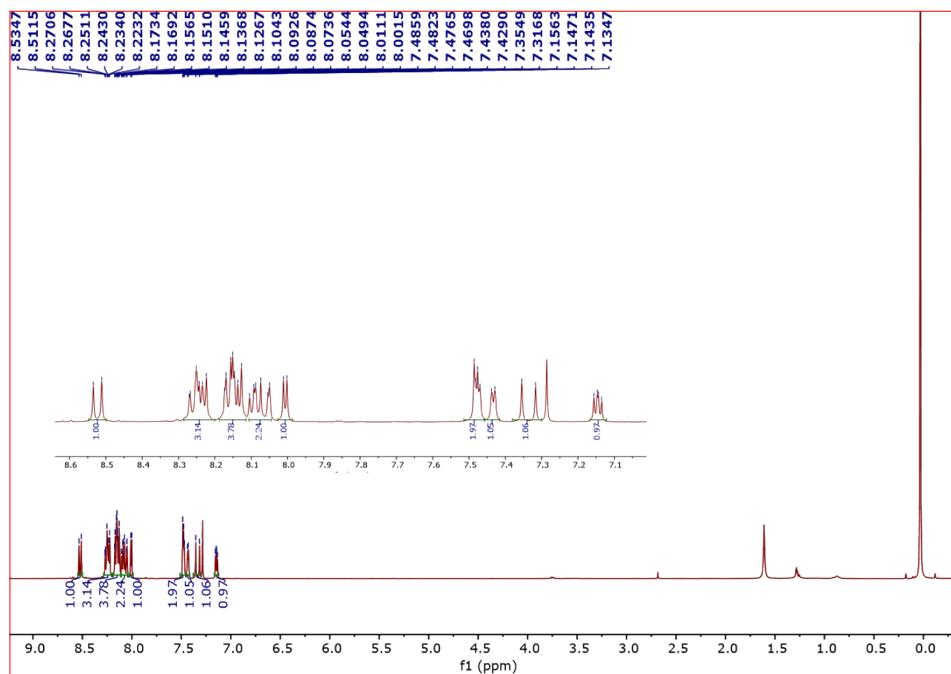


Figure S3. ^1H NMR of PySS in CDCl_3 solvent

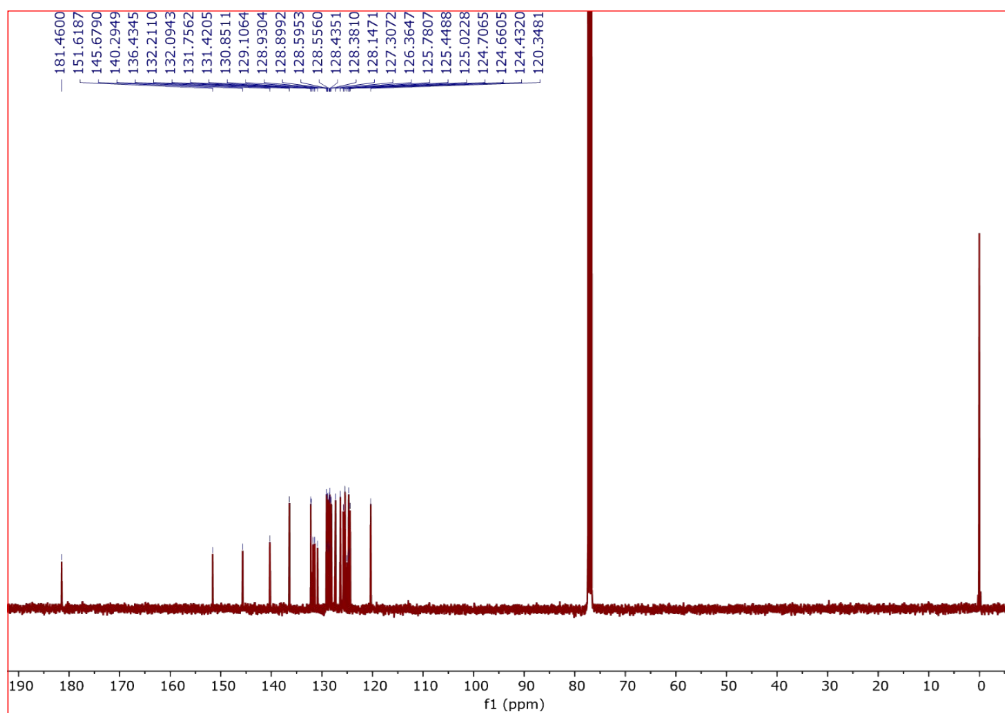


Figure S4. ^{13}C NMR spectra of PyS in CDCl_3 solvent

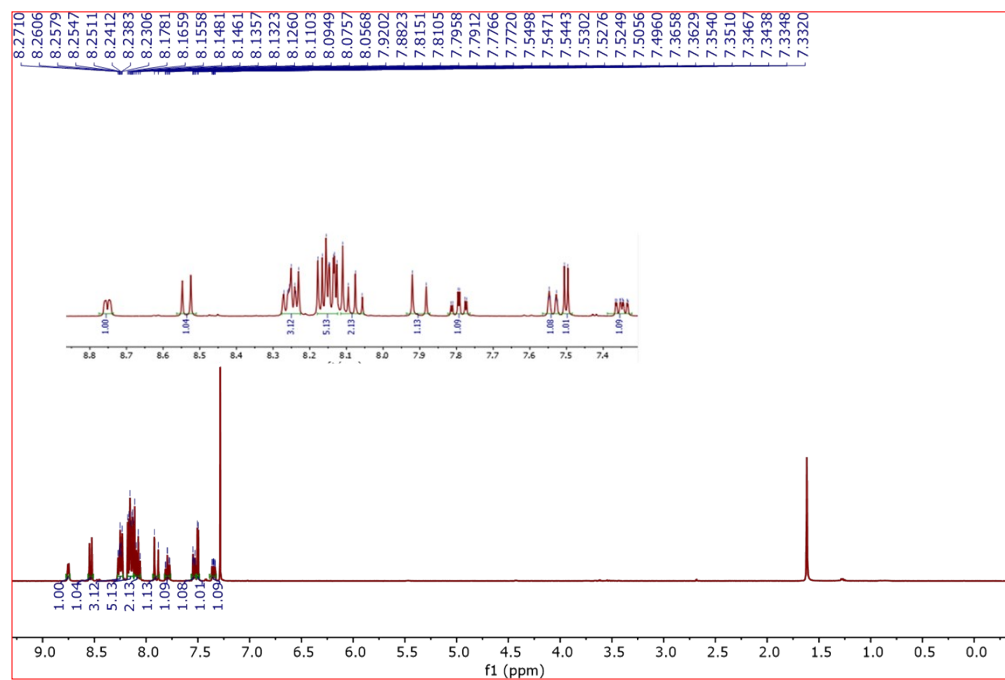


Figure S5. ^1H NMR spectra of PySP in CDCl_3 solvent

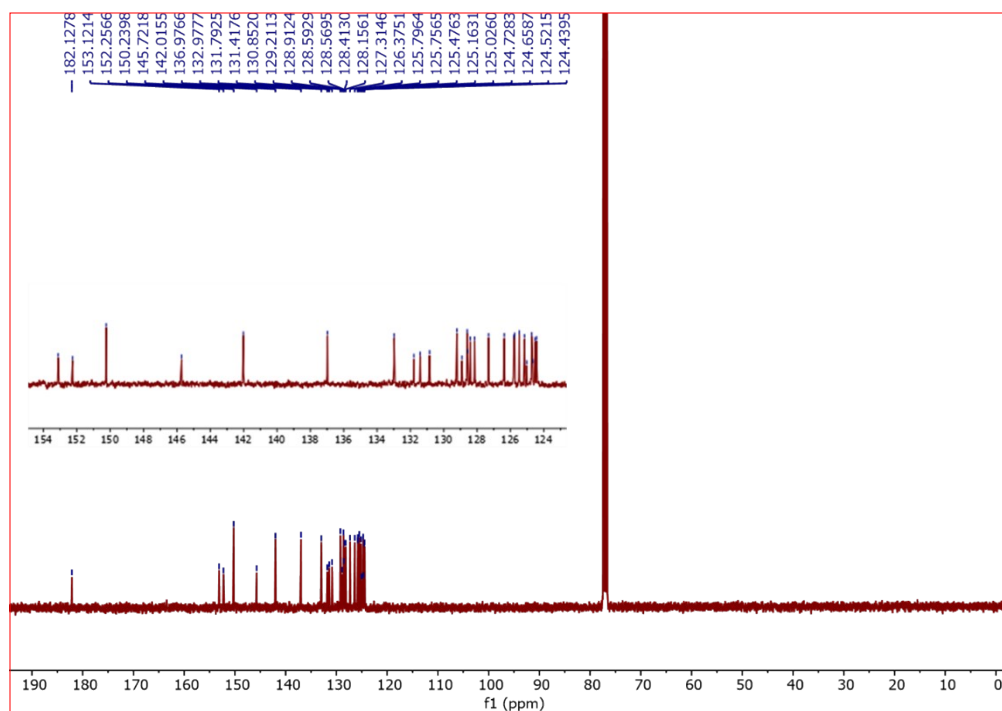


Figure S6. ^{13}C NMR spectra of PySP in CDCl_3 solvent

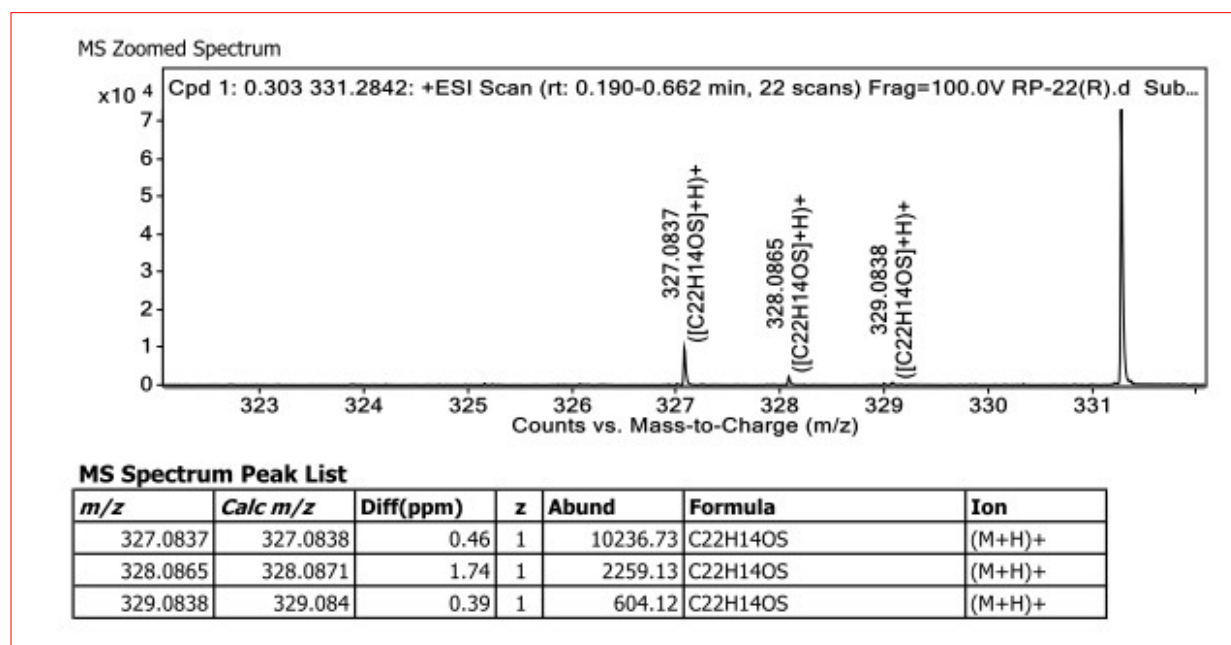


Figure S7. HRMS data of PyS

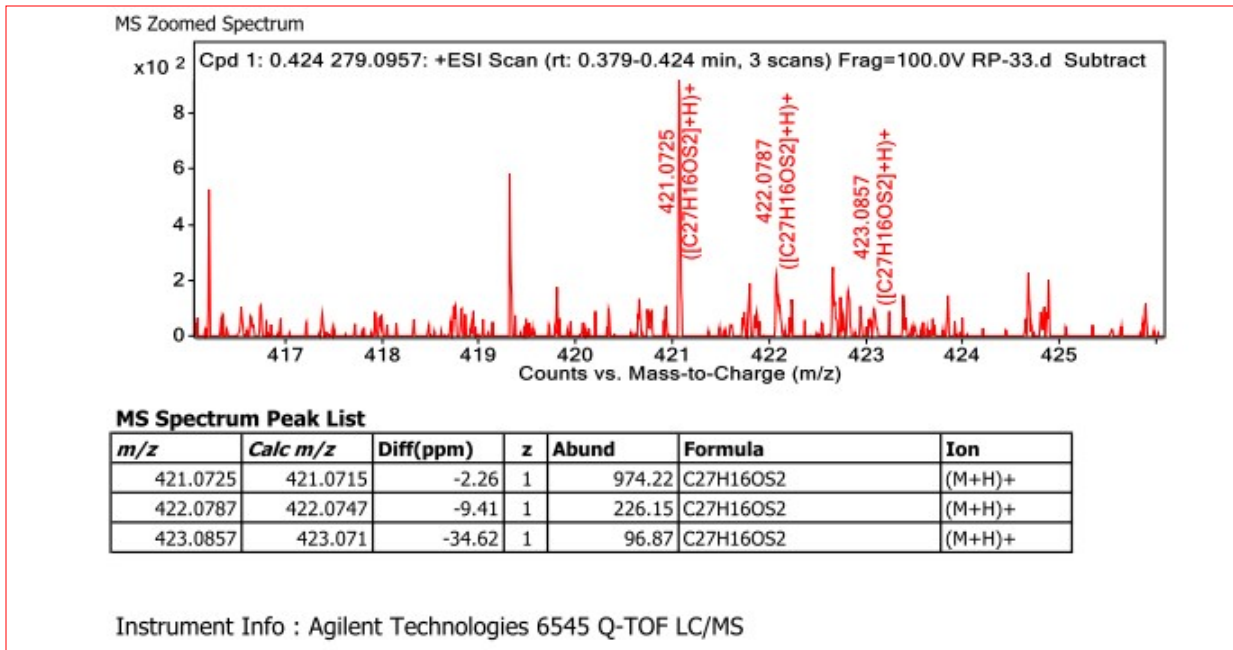


Figure S8. HRMS data of PySS

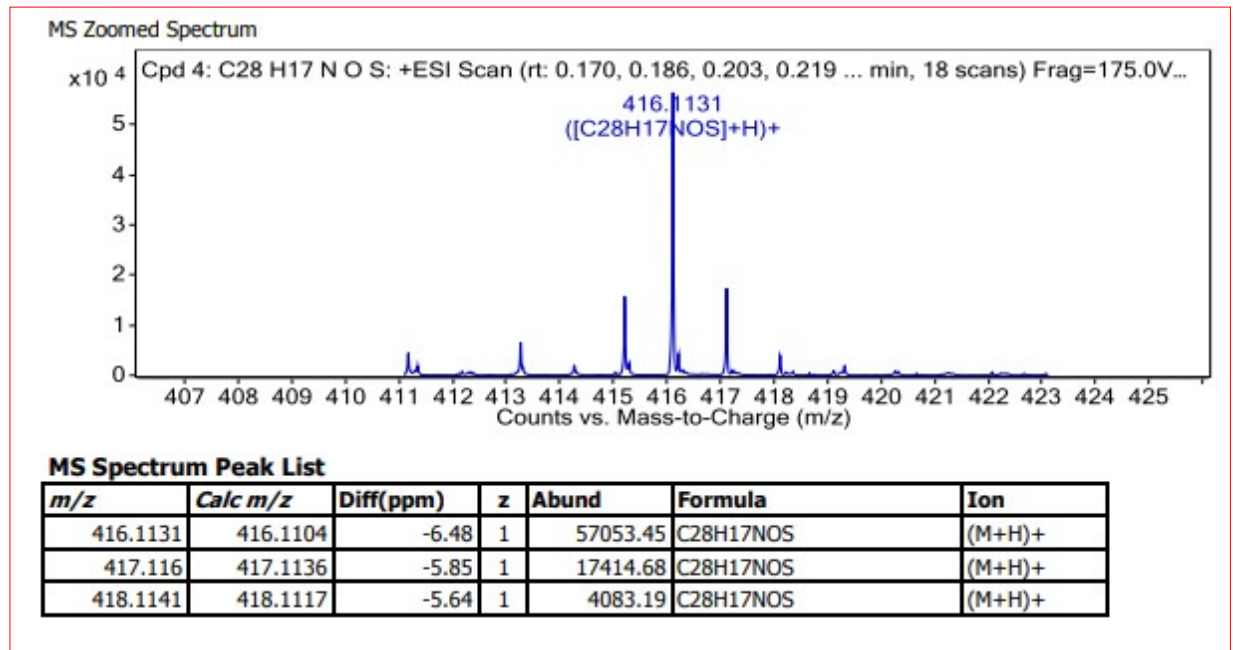


Figure S9. HRMS data of PySP

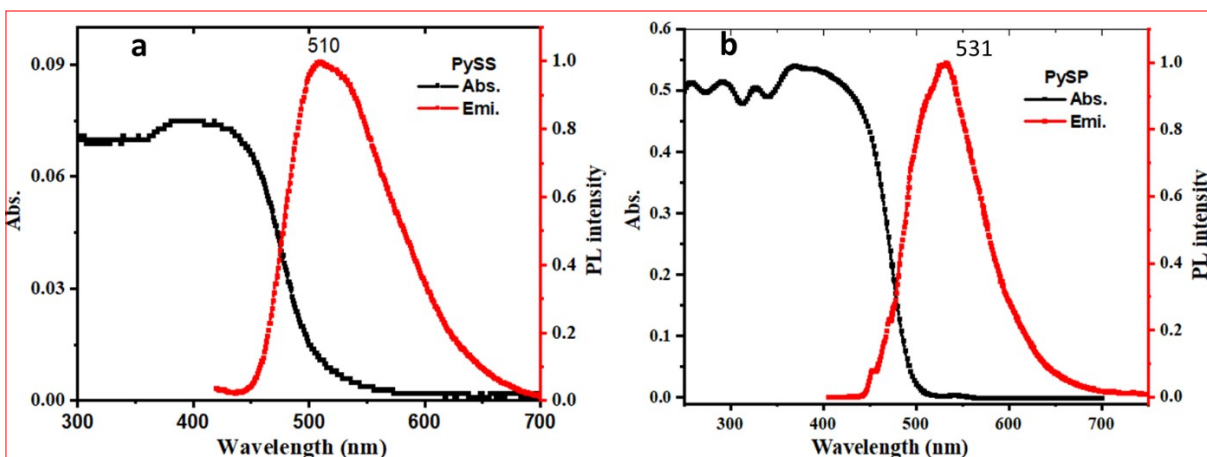


Figure S10. (a) Absorption spectra (black line) and emission (red line) in the solid state of PySS and PySP, respectively

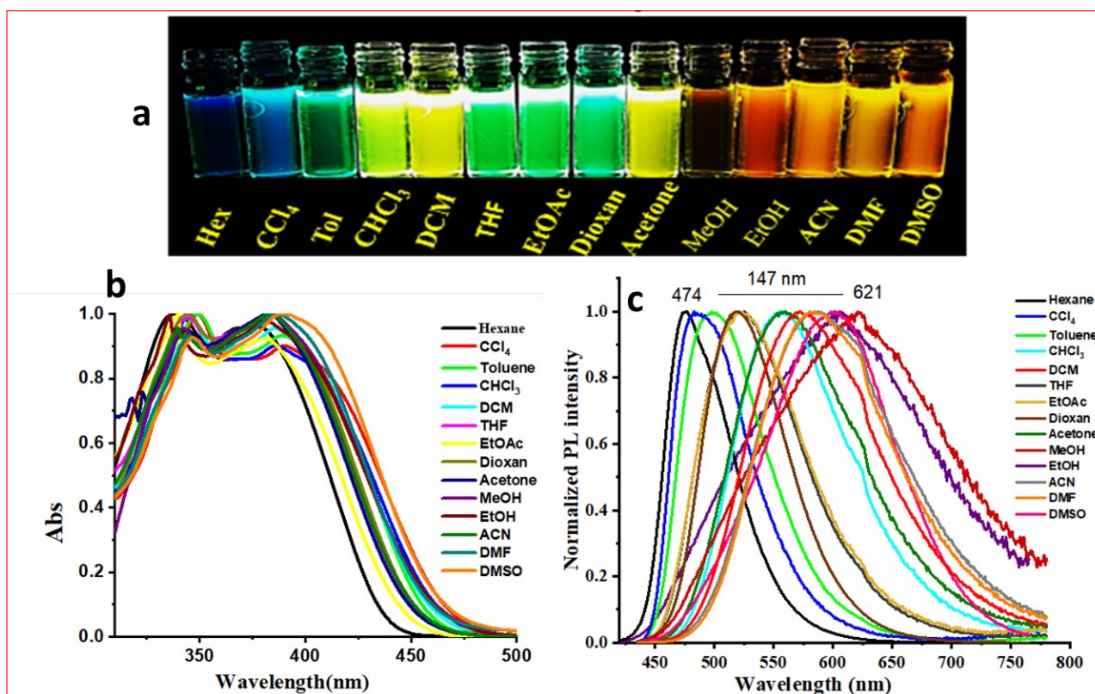


Figure S11. (a) Image of PySS in different solvents taken under 365 nm UV light excitation. (b) UV-visible spectrum of PySS in different solvents in wide ranges of polarities. (c) PL spectra of PySS in the same solvents used in absorption spectra.

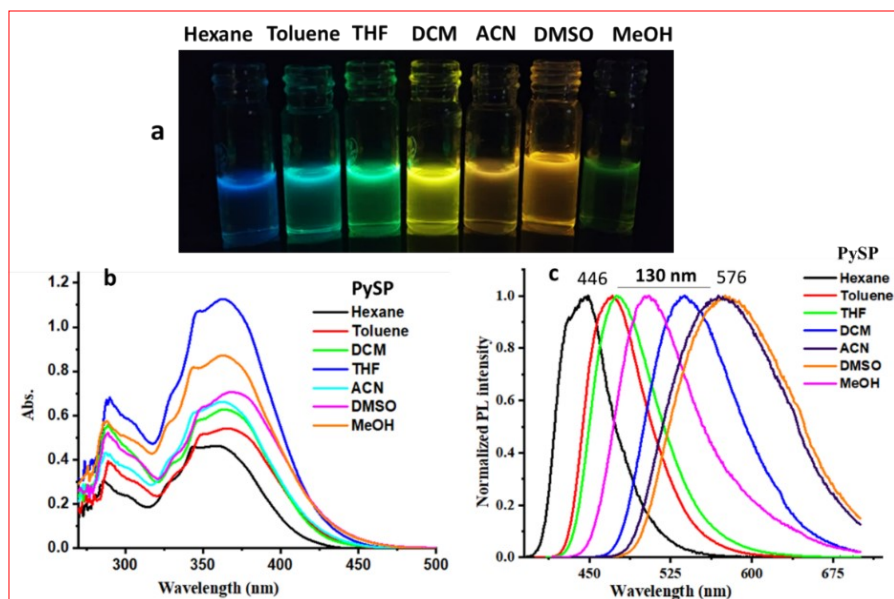


Figure S12. (a) Image of PySP in different solvents taken under 365 nm UV light excitation, (b) UV-visible spectrum of PySP in different solvents in wide ranges of polarities. (c) PL spectra of PySP in the same solvents used in absorption spectra

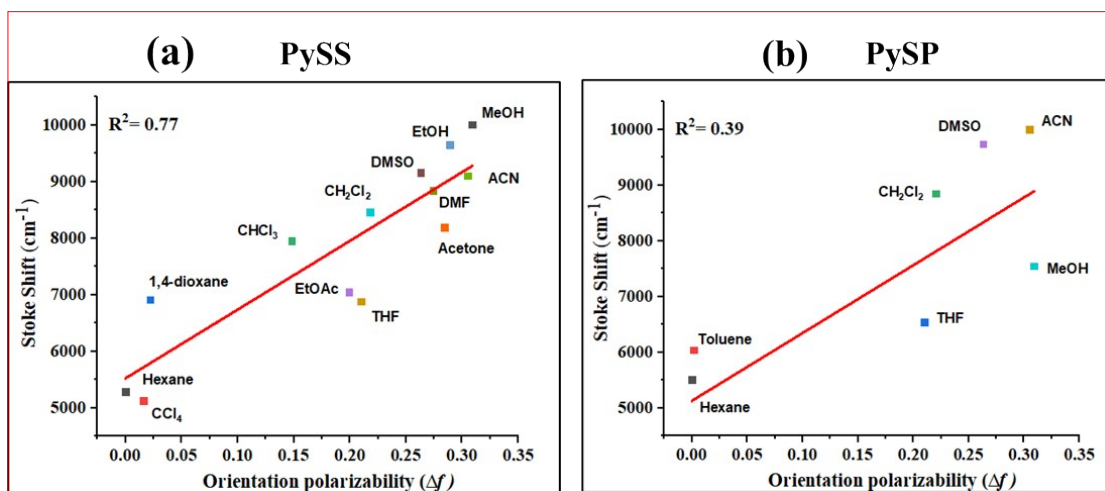


Figure S13. (a) Lippert–Mataga representation of orientation polarizability of PySS (a) and PySP (b) dissolved in different solvents

Table S1. Photophysical properties (absorption and emission) in different solvents (PySS)

S.NO.	Solvents	Absorption $\lambda_{\text{max.}}$ (nm)	Emission $\lambda_{\text{max.}}$ (nm)	Stokes shift (cm^{-1})
1	Hexane	379	474	5288
2	Carbon tetrachloride	389	486	5132
3	Toluene	389	490	5299
4	Chloroform	386	557	7953
5	Dichloromethane	385	571	8461
6	Tetrahydrofuran	384	522	6885
7	Ethyl acetate	381	521	7053
8	1,4-dioxan	383	521	6916
9	Acetone	382	556	8192
10	Methanol	383	621	10007
11	Ethanol	382	605	9649
12	Acetonitrile	383	588	9103
13	N,N'-dimethyl formamide	386	586	8842
14	Dimethyl sulfoxide	388	602	9162

Table S2. Photophysical properties in different solvents (PySP)

S.NO.	Solvents	Absorption $\lambda_{\text{max.}}$ (nm)	Emission $\lambda_{\text{max.}}$ (nm)	Stokes shift (cm^{-1})
1	Hexane	358	446	5511
2	Toluene	366	470	6046
3	Tetrahydrofuran	363	476	6540
4	Dichloromethane	364	537	8850
5	Methanol	364	502	7552
6	Acetonitrile	363	570	10004
7	Dimethyl sulfoxide	369	576	9739

Table S3. Quantum yields (Φ_f), and fluorescence lifetime (τ) of PySS and PySP samples before and after external stimuli.

Important parameters	Quantum yield (Φ_f), %		Lifetime $\langle\tau\rangle$, ns	
	PySS	PySP	PySS	PySP
Pristine	24.13	19.01	0.29	0.28
Ground	28.5	22.31	0.57	0.58
Press (12.5 ton)	13.03	9.45	0.93	0.94

Table S4. Non-covalent interactions present in crystal packing of PySS and PySP

S.NO.	Type of interaction	PySS	PySP
1	H-bonding	H26...O1 = 2.685 Å, H5...O1 = 2.597 Å,	O1...H6 = 2.579 Å O1...H4 = 2.645 Å
2	Inequivalent short contacts	C7...H27 = 2.883 Å C27...H1 = 2.796 Å	H3...H20 = 2.329 Å C26...H11 = 2.843 Å C23...H15 = 3.367 Å

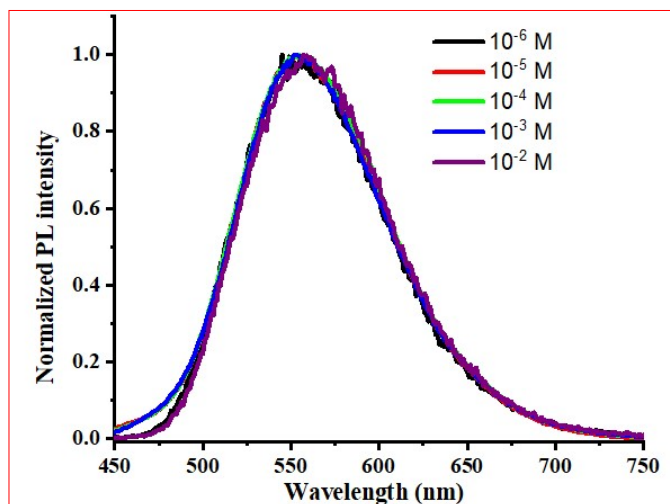


Figure S14. The normalized PL spectra of PySP in DCM solution with concentration from 1×10^{-6} M to 1×10^{-2} M

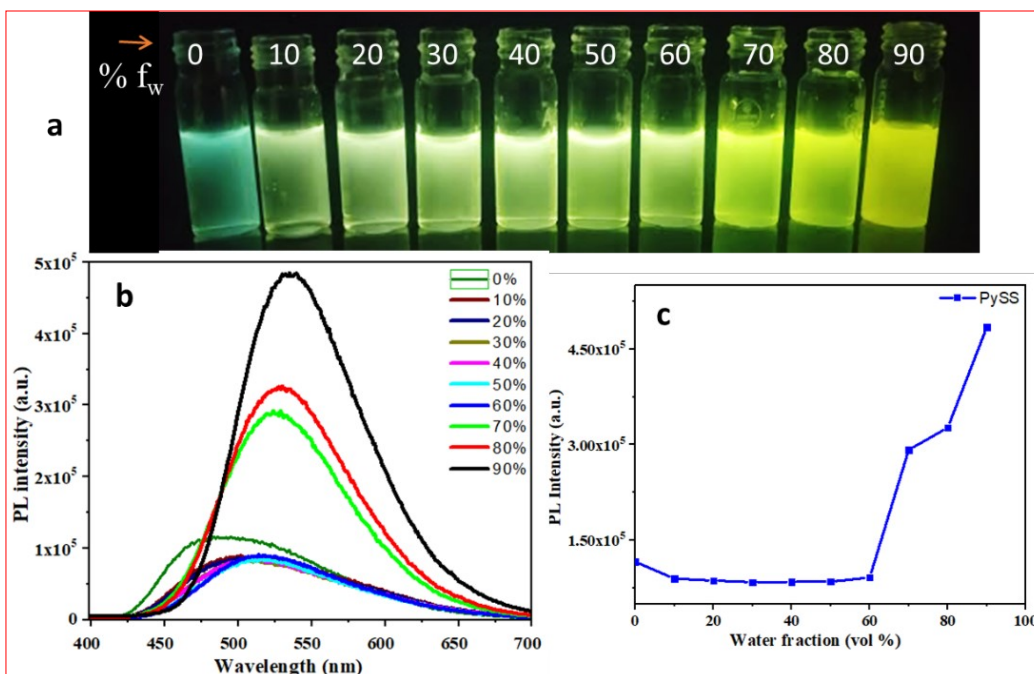


Figure S15. Aggregation-induced Emission study of PySS. (a) The image was taken at water percentage ($f_w = 0\%$ to $f_w = 90\%$) for PySS under a 365 nm UV excitation. (b) Emission spectra of PySS, ($\lambda_{ex} = 400$ nm) at different f_w in 100 μ M in THF. (c) Line plot of PL intensity versus volume of water fraction

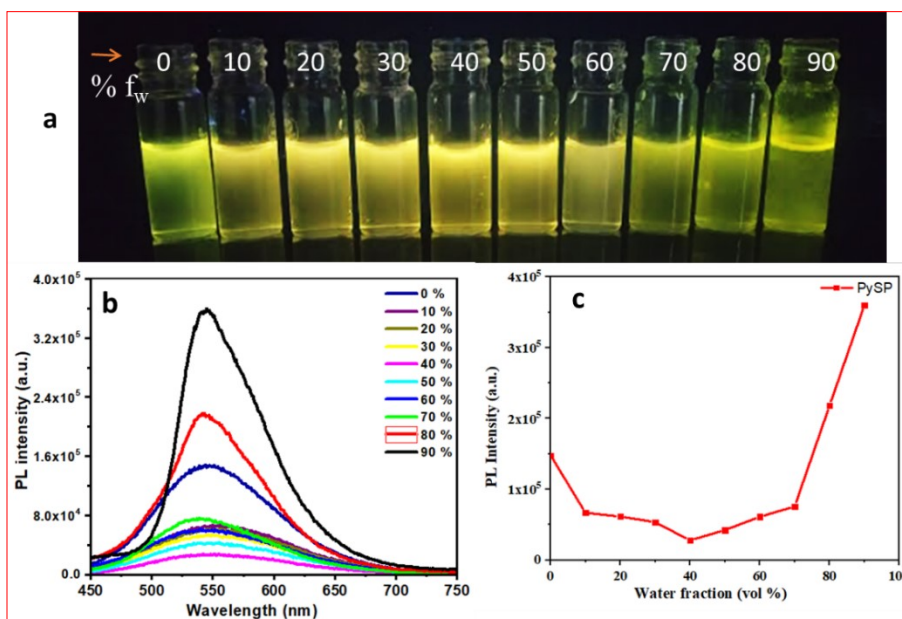


Figure S16 Aggregation-induced Emission study of PySP. (a) The image was taken at different water percentage ($f_w = 0\%$ to $f_w = 90\%$) for PySP under a 365 nm UV excitation. (b) Emission spectra of PySP, ($\lambda_{ex} = 400$ nm), at different f_w in 100 μ M in THF. (c) Line plot of intensity versus volume of water fraction

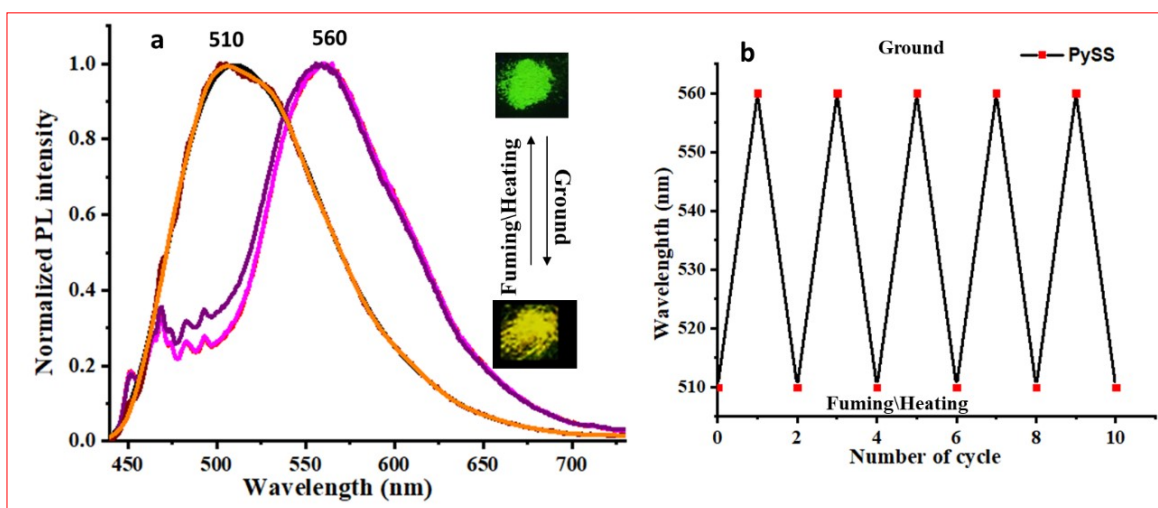


Figure S17. (a) PL spectra of PySS in pristine form and after grinding, (b) recoverability of emission property of ground sample of PySS after solvent (methanol fuming for 2 min) fumigation and heating (70-80 °C for 2 min). inset figure shows the emission color of pristine and ground sample under UV (365 nm) excitation

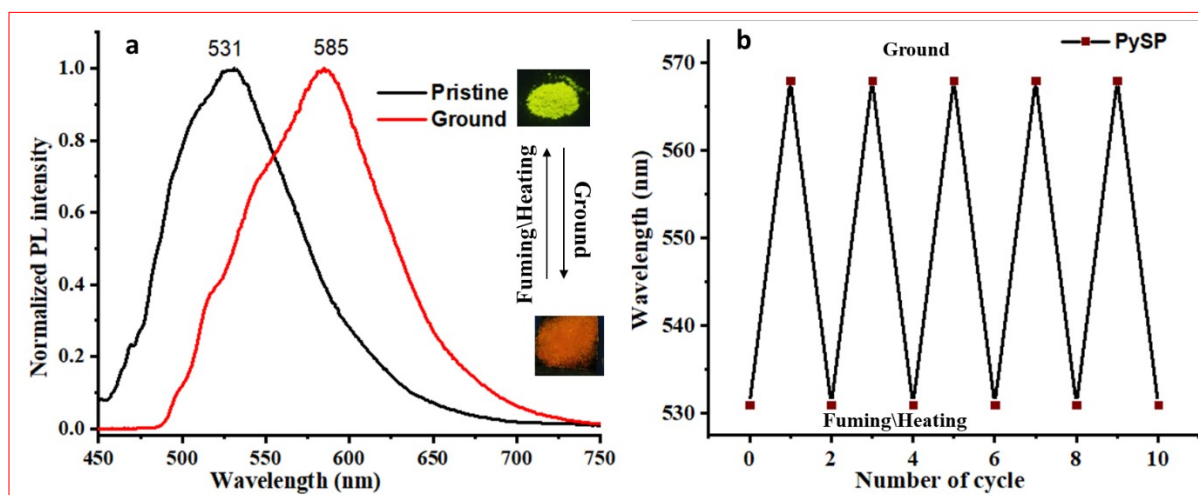


Figure S18. (a) PL spectra of PySP in pristine form and ground form, (b) recoverability of emission property of ground sample of PySP after solvent (methanol fuming for 2 min) fumigation and heating (70-80 °C for 2 min). inset figure shows the emission color of pristine and ground sample under UV (365 nm) excitation

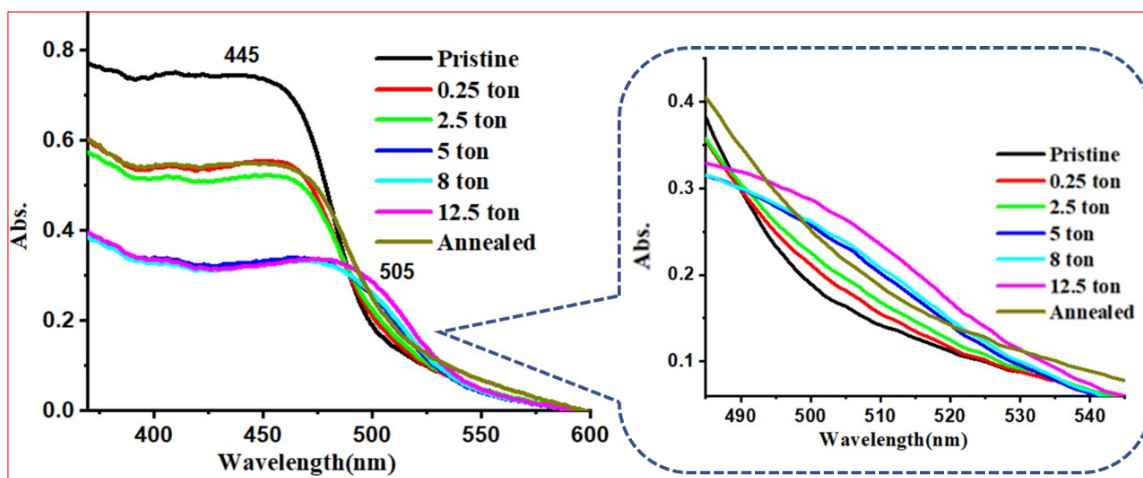


Figure S19. Solid state absorbance of PySS in pristine form and with gradual increasing hydraulic based pressure and the absorbance spectrum after releasing pressure with heating (annealed)

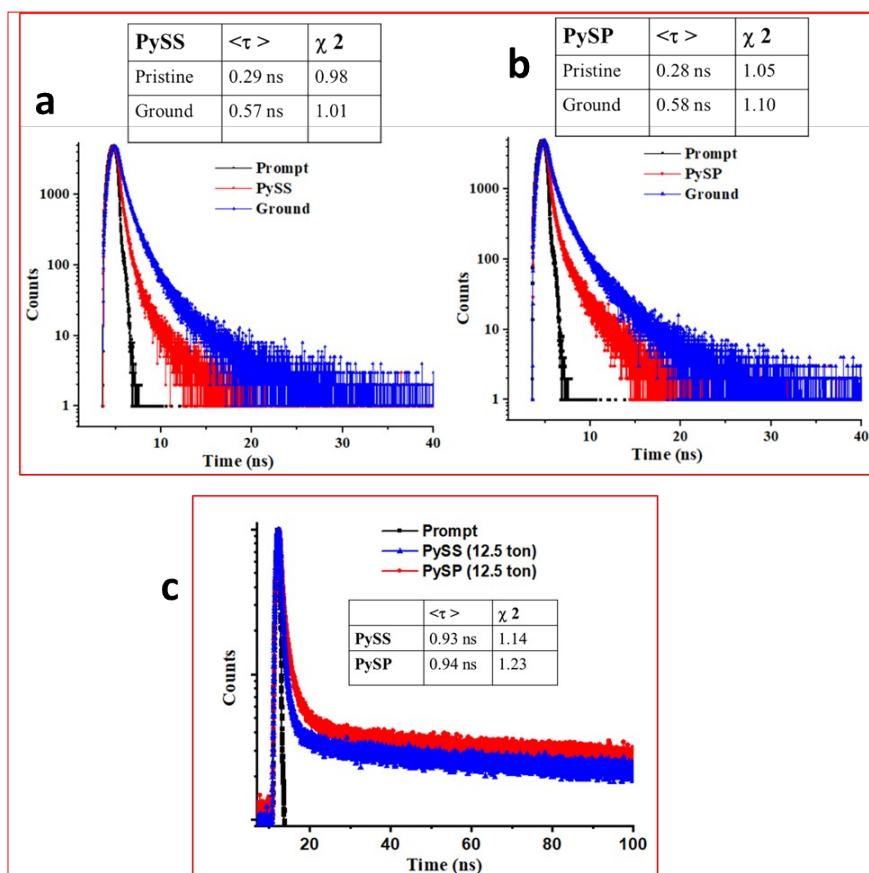


Figure S20. Lifetime plot of PySS and PySP in pristine form, ground form, and after applying pressure (12.5 ton), inset table shows the average lifetime with fitting parameter

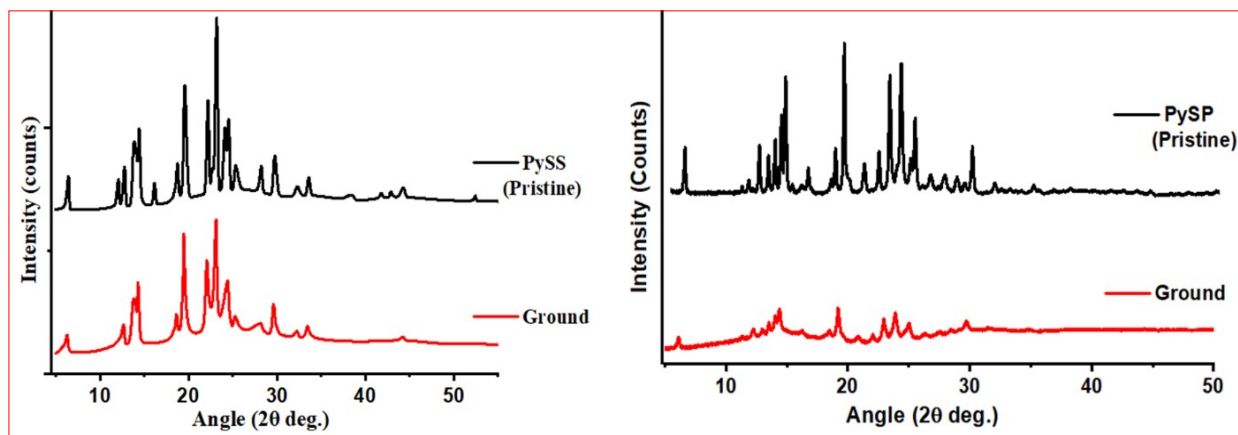


Figure S21. PXR D data of PySS and PySP in pristine and ground form

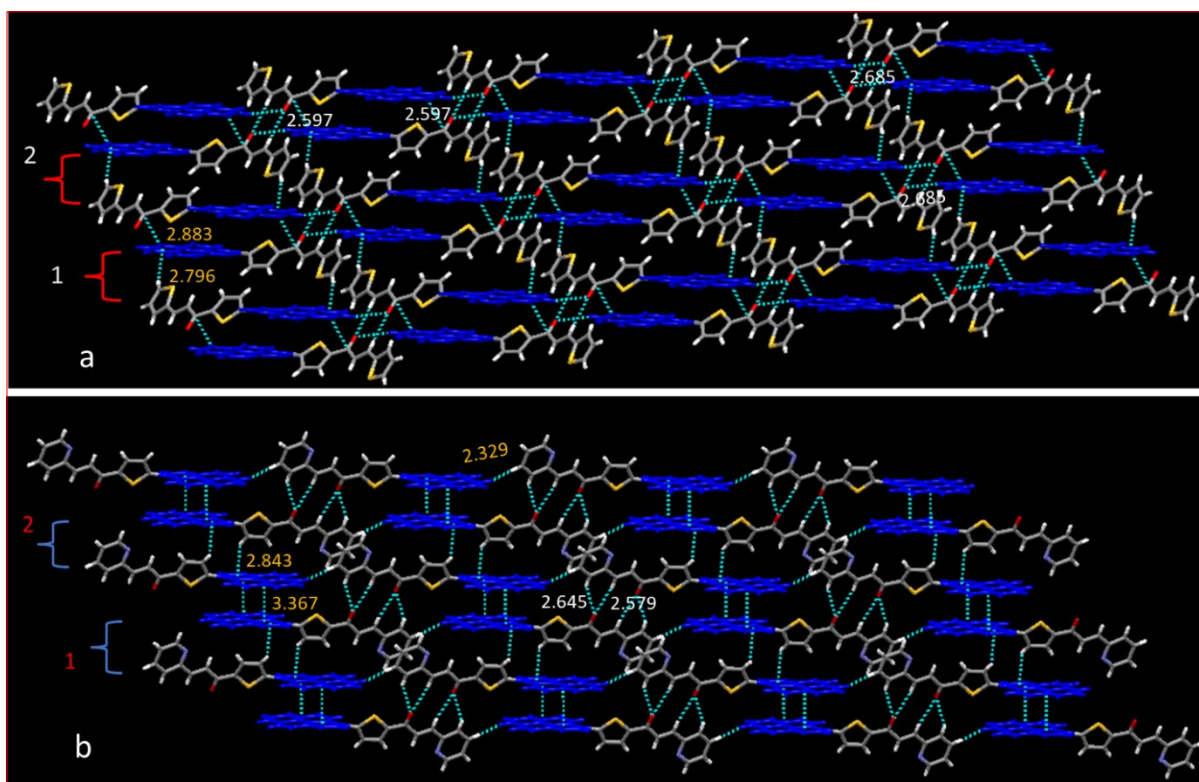


Figure S22 (a) crystal packing of m PySS showing interactions and short contacts between molecules and (b) Crystal packing of PySP with intermolecular with interactions between molecules

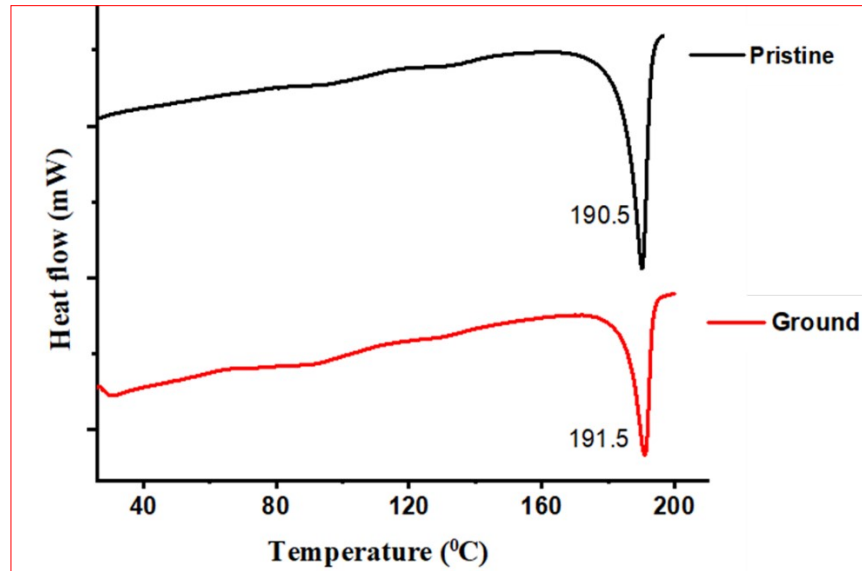


Figure S23. a) DSC analysis of PySS in pristine form and ground form, melting point observed at 190.5 °C for pristine sample and 191.5 °C for ground sample

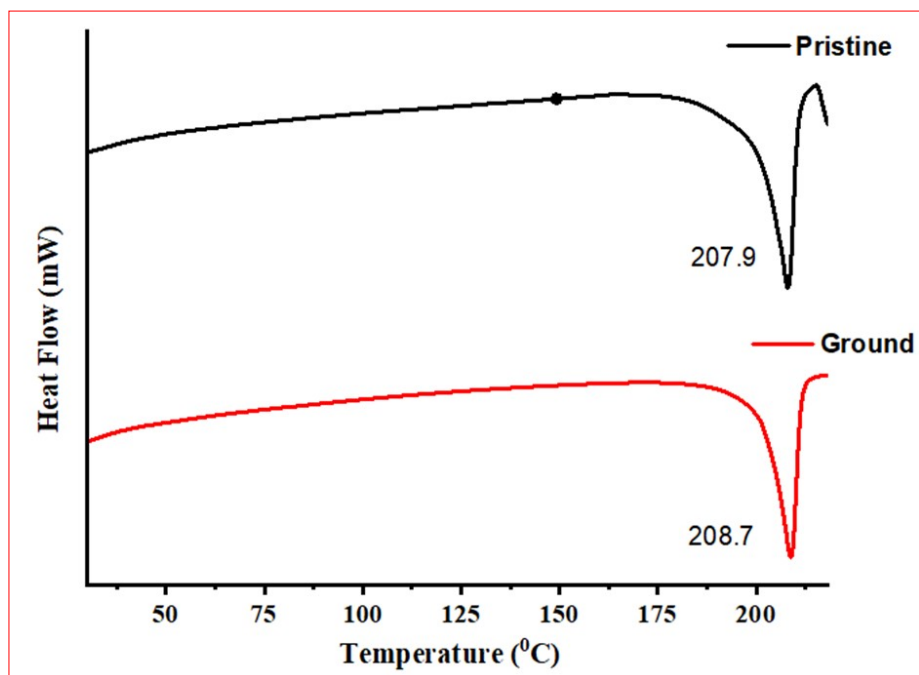


Figure S24. DSC of PySP in pristine form and ground form, melting point observed at 207.9 °C for pristine sample and 208.7 °C for ground sample

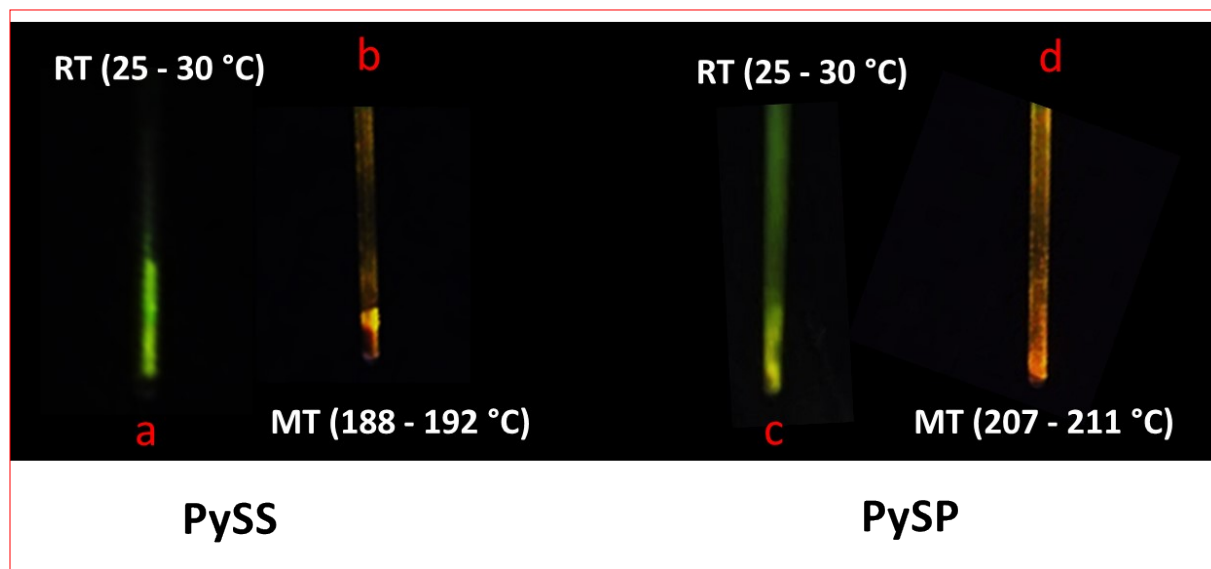


Figure S25. Filled the compounds in melting capillaries and captured the emission and after melting under UV (365 nm) excitation. a and c represent the image of compound filled in capillary at room temperature (RT) and b and d represent the capillary image at melting temperature (MT)

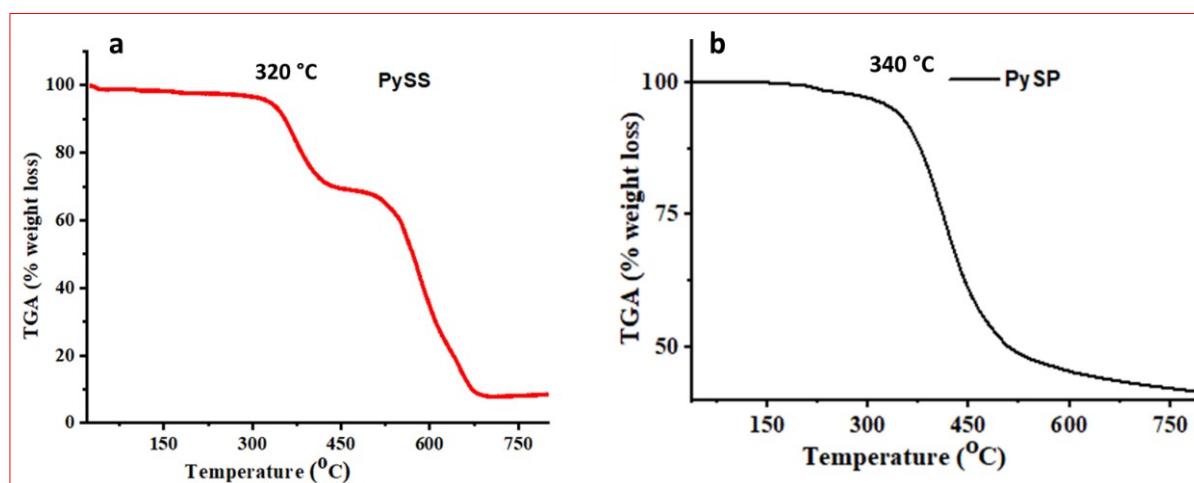


Figure S26. TGA analysis, a) thermogravimetric analysis of PySS and b) thermogravimetric analysis of PySP

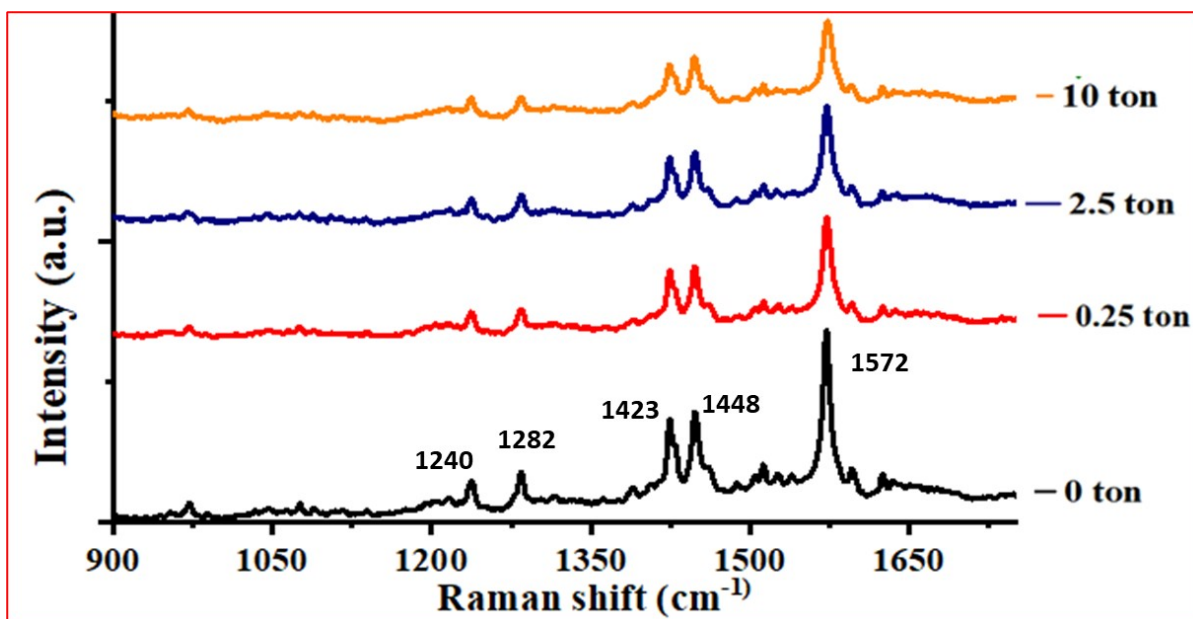


Figure S27. Raman analysis of PySS with increasing hydraulic pressure from 0 to 10 tons. It was observed that the peak at 1240 and 1282 cm^{-1} belongs to CH in-plane bending of the pyrene ring and that the peaks at 1423 cm^{-1} and 1448 cm^{-1} correspond to the C-C stretching for pyrene. The Raman frequency at 1572 cm^{-1} corresponds to the conjugated carbonyl (C=O) stretching frequency²

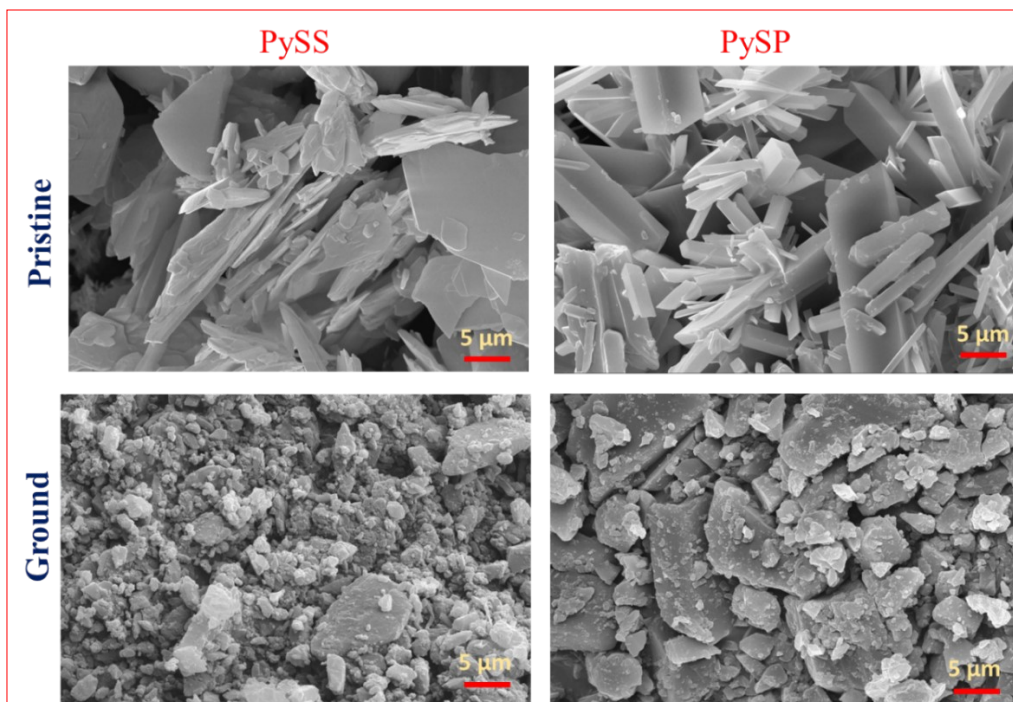


Figure S28. FESEM analysis of pristine phase and ground phase of PySS (left) and PySP (right)

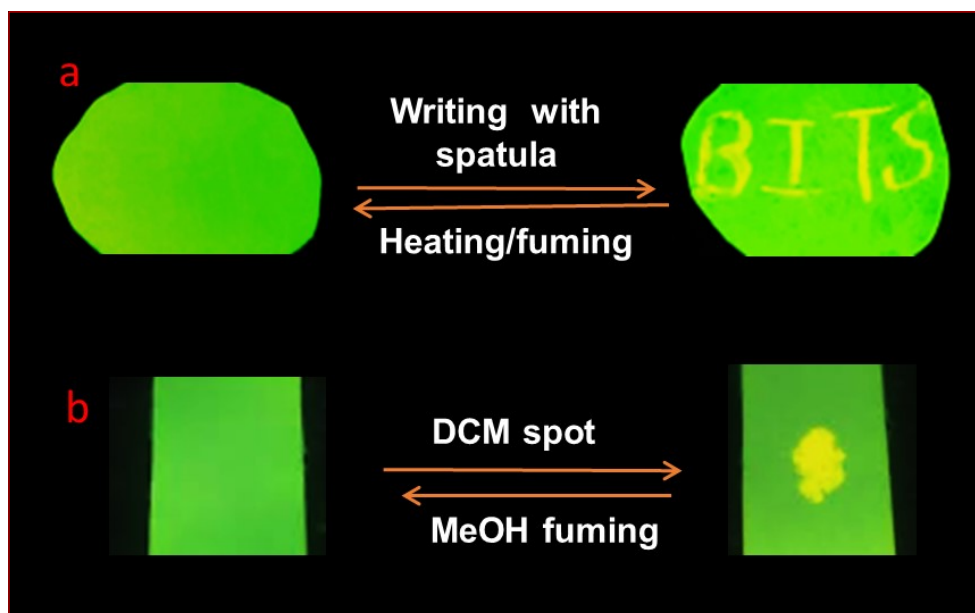


Figure S29. PySP is used to showcase rewritable paper and VOC detection. a, PySP dispersed filter paper left and after writing BITS by spatula (shearing force). b) PySP impregnated filter paper (left), put a drop of DCM (right). All image capture under UV excitation of 365 nm

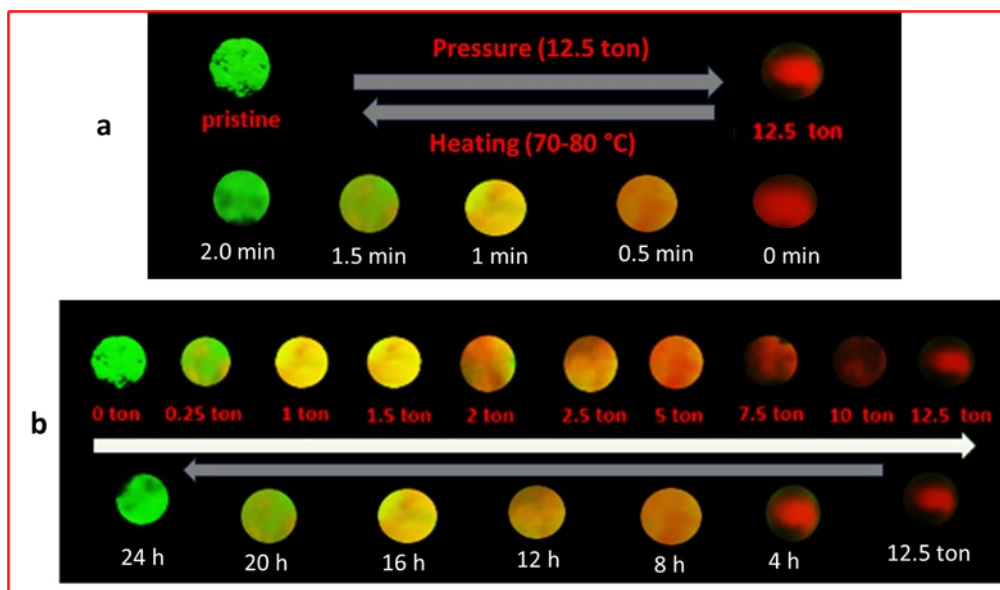


Figure S30. Emission images of PySS were taken under UV excitation (365 nm) with increasing amounts of hydraulic pressure and after releasing pressure with time. (a) shows images of the recovery process with heating (70-80 °C) at different times and (b) images of the recovery process with time without applying any external triggers up to 24 hr

Crystallographic Details

Single crystal X-ray diffraction data was collected on Rigaku XtaLABmini X-ray diffractometer equipped with Mercury CCD detector with graphite monochromatic Mo-K α radiation ($\lambda = 0.71073$ Å) at 100.0 (2) K using ω scans. The data was reduced using CrysAlisPro 41_64.93a software.³ The crystal structures were solved using Olex² package⁴ equipped with XT⁵ and were further refined using XL.⁶ Crystal packing and interaction diagrams were created using Mercury.⁷

Table S5. Crystallographic data table for PySS and PySP

Identification code	PySS
Empirical formula	C ₂₇ H ₁₆ O S ₂
Formula weight	420.52
<i>a</i> /Å	8.7703(3)
<i>b</i> /Å	9.0158(4)
<i>c</i> /Å	14.7970(4)
α /°	106.679(3)
β /°	92.045(3)
γ /°	113.849(4)
Temperature (K)	298
Wavelength	0.71073
Volume/Å ³	1009.60(8)
Space group	P -1
Hall group	-P 1
Formula weight	420.52
D _x ,g cm ⁻³	1.383
Z	2
μ /mm ⁻¹	0.281

F(000)	436.0
Radiation	Mo K α ($\lambda = 0.71073$)
h,k,l _{max}	13,13,22
Nref	7496
T _{min} , T _{max}	0.922, 0.948
Tmin'	0.919
Bond Precision	C-C = 0.0035 Å
Theta (max)	32.775
R (reflections)	0.0604 (3684)
wR2(reflections)	0.2122(6701)
S	1.033
Npar	274

Identification code	PySP
Empirical formula	C ₂₈ H ₁₇ NOS
Formula weight	415.48
Temperature/K	100.0(2)
Crystal system	Triclinic
Space group	<i>P</i> -1
<i>a</i> /Å	8.4274(7)
<i>b</i> /Å	8.9376(9)
<i>c</i> /Å	15.1384(11)
α /°	94.307(7)
β /°	105.783(7)
γ /°	112.410(8)

Volume/Å ³	993.68(16)
Z	2
ρ _{calc} /cm ³	1.389
μ/mm ⁻¹	0.185
F(000)	432.0
Crystal size/mm ³	0.23 × 0.22 × 0.22
Radiation	Mo Kα (λ = 0.71073)
2θ range for data collection/°	5.032 to 50.092
Index ranges	-10 ≤ h ≤ 10, -10 ≤ k ≤ 10, -18 ≤ l ≤ 18
Reflections collected	10602
Independent reflections	3508 [R _{int} = 0.0318, R _{sigma} = 0.0362]
Data/restraints/parameters	3508/0/280
Goodness-of-fit on F ²	1.112
Final R indexes [I ≥ 2σ (I)]	R ₁ = 0.0706, wR ₂ = 0.1883
Final R indexes [all data]	R ₁ = 0.0848, wR ₂ = 0.2350
Largest diff. peak/hole / e Å ⁻³	1.13/-0.57

1. Bhatta, R. P.; Kachwal, V.; Climent, C.; Joshi, M.; Alemany, P.; Choudhury, A. R.; Laskar, I. R., Tunable emission in the visible range from a single organic fluorophore through time-controlled morphological evolution. *Journal of Materials Chemistry C* **2023**, *11* (33), 11399-11408.
2. Xie, Y.; Wang, X.; Han, X.; Xue, X.; Ji, W.; Qi, Z.; Liu, J.; Zhao, B.; Ozaki, Y., Sensing of polycyclic aromatic hydrocarbons with cyclodextrin inclusion complexes on silver nanoparticles by surface-enhanced Raman scattering. *Analyst* **2010**, *135* (6), 1389-1394.
3. Miclaus, M. O.; Kacso, I. E.; Martin, F. A.; David, L.; Pop, M. M.; Filip, C.; Filip, X., Crystal structure and desolvation behaviour of the tadalafil monosolvates with acetone and methyl ethyl ketone. *Journal of Pharmaceutical Sciences* **2015**, *104* (11), 3782-3788.
4. Dolomanov, O. V.; Bourhis, L. J.; Gildea, R. J.; Howard, J. A.; Puschmann, H., OLEX2: a complete structure solution, refinement and analysis program. *Journal of applied crystallography* **2009**, *42* (2), 339-341.
5. Sheldrick, G. M., Crystal structure refinement with SHELXL. *Acta Crystallographica Section C: Structural Chemistry* **2015**, *71* (1), 3-8.
6. Sheldrick, G. M., A short history of SHELX. *Acta Crystallographica Section A: Foundations of Crystallography* **2008**, *64* (1), 112-122.
7. Macrae, C. F.; Bruno, I. J.; Chisholm, J. A.; Edgington, P. R.; McCabe, P.; Pidcock, E.; Rodriguez-Monge, L.; Taylor, R.; Streek, J.; Wood, P. A., Mercury CSD 2.0—new features for the visualization and investigation of crystal structures. *Journal of Applied Crystallography* **2008**, *41* (2), 466-470.